Original Article

Indentation of composite sandwich panels with aluminum foam core: An experimental parametric study

Zhibin Li[1,2], Zhijun Zheng[1], Jilin Yu[1] and Jie Yang[1]

Abstract

Quasi-static indentation tests were carried out to investigate the mechanical responses of sandwich panels with composite face sheets and aluminum foam core. The energy absorption, specific energy absorption and energy-absorbing effectiveness factor of rigid-supported composite sandwich panels were evaluated and compared. The deformation of upper face sheets, foam cores and lower face sheets was captured. The effects of several key parameters, including the face sheet thickness, the core thickness and relative density, and the indenter nose shape, on the energy absorption behavior of the rigid-supported sandwich panels were explored. The dependency of the load–displacement response of sandwich panels on boundary conditions was also discussed. It was found that the rigid-supported sandwich panels absorb the greatest energy and own the highest energy absorption efficiency, while fully fixed panels absorb the least energy and own the lowest energy absorption efficiency.

Introduction

Composite sandwich panels made of composite face sheets and foam core have many advantages, such as lightweight, high specific strength, and stiffness.[1,2] However, one of the main concerns in the application of composite structures is the fact that composite sandwich panels are susceptible to indentation failure due to localized loading,[3] such as runway debris, hailstones, and accidentally dropped heavy tools. The load-carrying capacity of the sandwich panels may be significantly reduced by the presence of such damages.[4] Hence, it is of practical importance to make a good understanding of the indentation responses of sandwich structures.

In recent years, a number of studies have shown that localized impact loading on a sandwich structure can result in the generation of local damage, which can lead to significant reductions in its load-carrying capacity.[5,6] However, most of the previous researches on composite sandwich panels were focused on structures with polymer foam cores[7,8] or honeycomb cores.[9,10] Recently, some research attention has turned to replacing the

polymer foams with metal foams.[11–14] In engineering practice, metal foams may replace polymer foams where multi-functionality is important. For example, it can act as a structural component in a sandwich panel and also as a cooling system or acoustic damper.[15] Ruan et al.[11] conducted experimental studies on sandwich panels with ALPORAS aluminum foam core and aluminum face-sheets using an MTS universal testing machine. Effects of face-sheet thickness, core thickness, boundary conditions, adhesive, and surface condition of face-sheets were discussed. Mohan et al.[12]

[1]CAS Key Laboratory of Mechanical Behavior and Design of Materials, University of Science and Technology of China, Hefei, PR China
[2]College of Science, National University of Defense Technology, Changsha, PR China

Corresponding author:
Zhijun Zheng, CAS Key Laboratory of Mechanical Behavior and Design of Materials, University of Science and Technology of China, Hefei, Anhui 230026, PR China.
Email: zjzheng@ustc.edu.cn

experimentally studied sandwich panels comprising aluminum foam cores and various types of face-sheets (whose behavior represents elastic, elastic-ideally plastic, and elastic-plastic strain hardening) under quasi-static indentation. Results show that the indentation behavior is strongly dependent on the type and thickness of the face sheets used. In this study, experiments are carried out to make a good understanding of the indentation response of sandwich structures with composite face sheets and aluminum foam cores.

For the reason that inertia and wave propagation effects are negligible in the case of low-velocity impact, several studies[16,17] show a similarity between quasi-static indentation and drop weight impact testing. It was found that the resistance forces of the sandwich panels were very similar in both quasi-static indentation and low-velocity impact indicating that quasi-static indentation can be used to study low-velocity impact responses.[16] In our previous work,[18] a preliminary research on the quasi-static perforation and low-velocity impact behavior of sandwich panels with aluminum foam core and woven fabric face sheets was carried out. It was found that the resistance forces of the sandwich panels showed a similarity between quasi-static perforation and drop weight impact tests. The same conclusion can be deduced for the indentation cases,[8] indicating that it is applicable to use quasi-static indentation to study the low-velocity impact indentation responses.[2] Moreover, the need for quasi-static indentation test method for modeling low-velocity impact events to sandwich composites has been proved to be very beneficial.

Quasi-static indentation tests are conducted on the sandwich panels with closed-cell aluminum foam cores and composite face sheets in this study. The indentation responses of the sandwich panels are investigated and the deformation and failure modes observed during indentation are described in detail. Three kinds of boundary conditions are considered and indenters with different nose shapes are used. An experimental parametric study is carried out to investigate the effects of various geometric parameters, such as the face sheet thickness, the core thickness and relative density, the indenter nose shape, as well as the boundary conditions on the energy absorption performances of sandwich panels.

Experiments

Materials and structures

The sandwich panels used here are similar to those used in our previous study on perforation behavior.[18] Thus, materials and structures are briefly described below.

The face sheets of all panels are made of woven-glass fabric laminates, in which the fabric is E-glass fiber 7628 cloth with the filament diameter of about 10 μm, and the matrix is thermosetting phenolic resin. The face sheets have a fiber volume ratio of 0.60 and a density of 2.31 g/cm^3 and comprise $0°/90°/0°$ configuration with the fiber direction parallel to one side of the panel. Three different thicknesses of the upper face sheet ($H_{uf} = 1.2$, 1.5, and 2.0 mm) are considered while all the lower face sheets have an identical thickness of $H_{lf} = 2.5$ mm. The face sheet material is found to be linearly elastic till fracture with an ultimate stress of 330 MPa at an ultimate strain of 1.35%, regardless of the thickness.[18]

A closed-cell aluminum foam with an average cell size of ~3 mm produced by liquid state processing using TiH$_2$ as a foaming agent is used as the core material. Three different relative densities, namely, $\rho = 14.1\%$, 19.6%, and 23.3%, are used in this study and their plateau stress have been experimentally determined as $\sigma_{pl} = 5.82$, 7.31, and 8.98 MPa, respectively, as done in Li et al.[18]

Sandwich specimens were manufactured by utilizing a two-component impact-resistant adhesive SA102 to glue the face sheets and the foam core together.

The specimens are square plates 150×150 mm^2 in dimensions, and are named as <upper face sheet thickness in mm>-<core thickness in mm>-<lower face sheet thickness in mm>-<repetition number> in the present study.

Indentation tests

To investigate the mechanical behavior of sandwich panels exposed to localized loads, an MTS809 material test system was used to perform the quasi-static indentation tests. Three different indenters, i.e. a conical-nosed, a hemispherical-nosed, and a flat-ended indenter, with an identical diameter are used for comparison. Figure 1 illustrates the geometry and dimensions of the indenters.

Sandwich panels were placed on the top of a rigid substrate without any clamping device (Figure 2(a)), and the indentation load was applied at the center mainly through a steel conical-nosed indenter. All the tests were carried out under displacement control with a constant loading rate of 0.02 mm/s and the indentation force–displacement histories were recorded.

Because of non-conduciveness of the adhesive, electron discharge machining (EDM) fails to machine the indented specimens. Thus, the specimens after tests were sectioned by a bench saw at low speeds for observing the damage zone.

An important issue in measuring the mechanical properties of foams is the effect of the specimen size,

relative to the cell size. The size effect is also particularly important for foam core sandwich panels, as in some components the foam core may have dimensions of only a few cell diameters. The size effect of sandwich beams has already been experimentally demonstrated for shear failure of four-point bending.[19] In the present study, the ratio of the indenter diameter to the average cell size is about 10; thus, no significant effect of cell size on perforation response will be noticed according to Andrews et al.[20] The size effect can be avoided if the foam plate has at least eight cell diameters in thickness according to Tekoglu et al.[21] However, the thin and stiff face sheets will give a better distribution of load throughout the area when subjected to loads, which would lead to a lower localized mean load and diminish the size effects. Moreover, in real sandwich components, the foam cores may just have limited cell diameters across the thickness of the panels despite the foam core is only about five cell diameters in thickness in this study.
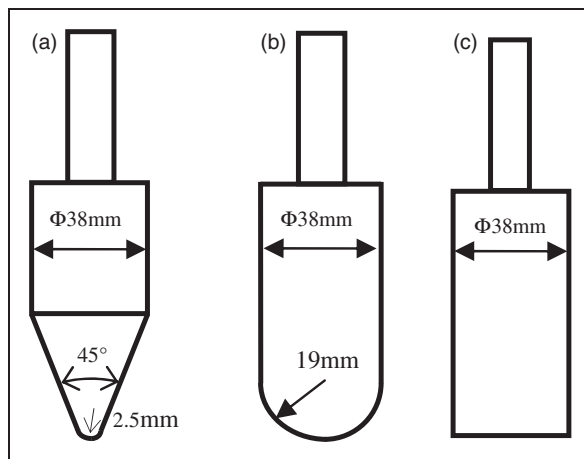

Figure 1. Geometry and dimensions of the indenters: (a) conical-nosed (CNP); (b) hemispherical-nosed (SEP); and (c) flat-ended (FEP).

Results

Deformation features of face sheets and core

Localized deformation in the upper face sheet was observed from the beginning of each test. For the rigid-supported (RS) specimens loaded by different indenters, i.e. conical-nosed, hemispherical-nosed, and flat-ended indenters, differences could be found in the damage patterns of the upper face sheets of the specimens, as shown in Figure 3. It should be noted that the surface of the laminates is covered by a layer of silver-colored twill glass fabrics, so the visual patterns are not the actual fiber orientations. The cross-sectional views of the RS specimens after tests are shown in Figure 4. The photographs of damaged specimens for other support conditions, such as fully clamped sandwich panels, can be found in our previous paper.[18] Damage mode-I in Figure 3(a) and Figure 4(a) was observed in most cases of sandwich panels with a thin upper face sheet indented by the hemispherical indenter, while damage mode-II in Figures 3(b) and Figure 4(b) was observed in sandwich panels with a thick upper face sheet. For damage mode-I, partial penetration through the thickness of the face sheet happened over a larger area in a circular manner after large deformation of the face sheet. Cracks occurred aligned along the circumferential edge of the indenter. For damage mode-II, the hemispherical indenter produced cracks over a much large area under the indenter in a square manner that is parallel and perpendicular to the fiber direction, and the face sheet tore into four pieces, as can be seen in Figure 3(b).

It is interesting to note that in Figure 3(c) and Figure 4(c) the flat-ended indenter punches through the face sheet around the circumferential edge of the indenter while crushing the foam core underneath. For the conical indenter with a sharper nose, an initial perforation of the face sheet without considerable crushing of foam core was observed, followed by the formation of

Figure 2. Photographs of the boundary conditions: (a) placed on the top of a rigid substrate without any clamping device (RS); (b) placed on a specially designed frame with panel edges SS; (c) fully clamped (FF).
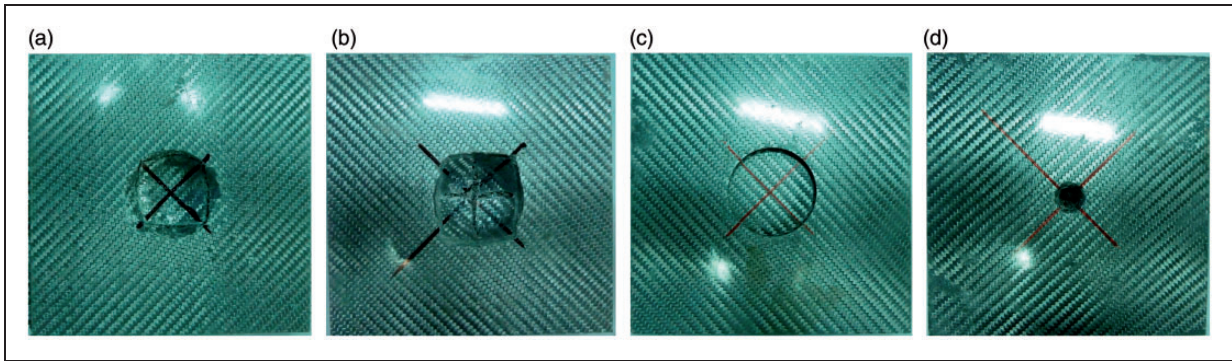
Figure 3. Photographs of post-test RS sandwich specimens: (a) face-sheet damage by a hemispherical-nosed indenter (mode-I); (b) face-sheet damage by a hemispherical-nosed indenter (mode-II); (c) face-sheet damage by a flat-ended indenter (mode-III); and (d) face-sheet damage by a conical-nosed indenter (mode-IV).

Figure 4. Cross-sections of post-test RS sandwich specimens: (a) face-sheet damage by a hemispherical-nosed indenter (mode-I); (b) face-sheet damage by a hemispherical-nosed indenter (mode-II); (c) face-sheet damage by a flat-ended indenter (mode-III); and (d) face-sheet damage by a conical-nosed indenter (mode-IV).
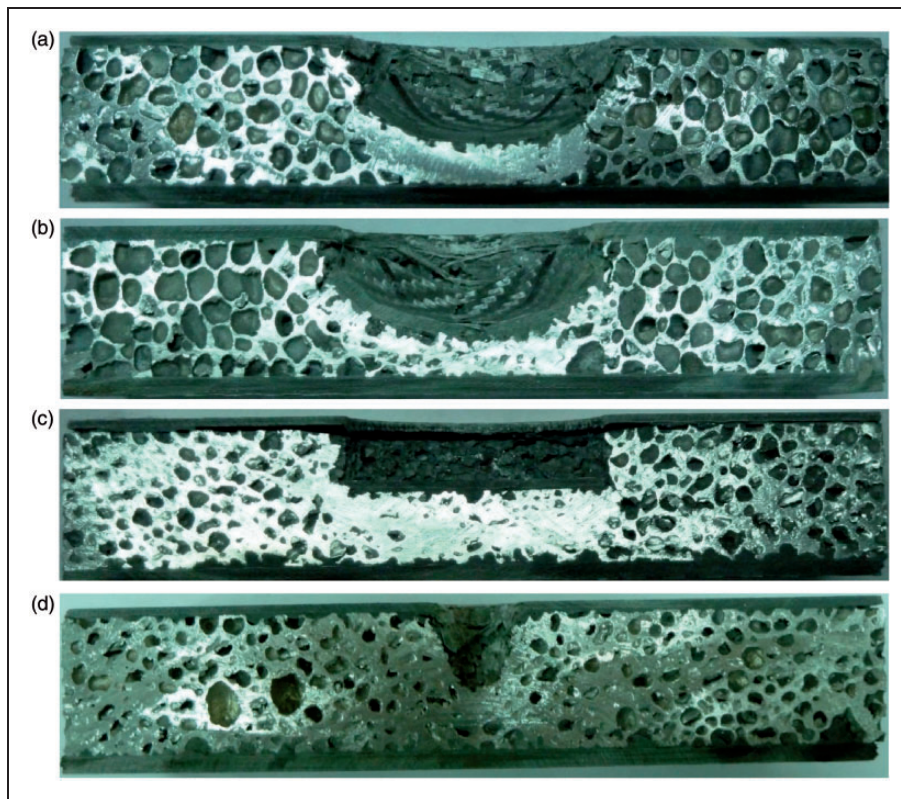
circular cracks which correspond to the striker diameter and then the upper face sheets tore into several pieces, as seen in Figures 3(d) and Figure 4(d).

Load response

Two or more sandwich specimens were tested for every selected case. The results are consistent with a variation of less than 5% for both the first peak load and the indentation displacement at failure (data not shown), which is sufficient to ensure the consistency of the tests. Figure 5 shows a typical measured force–displacement curve for indentation of RS sandwich panels under a hemispherical-nosed indenter, which is similar to the stress–strain curve of closed-cell aluminum foams under uniaxial loading. The load responses are different
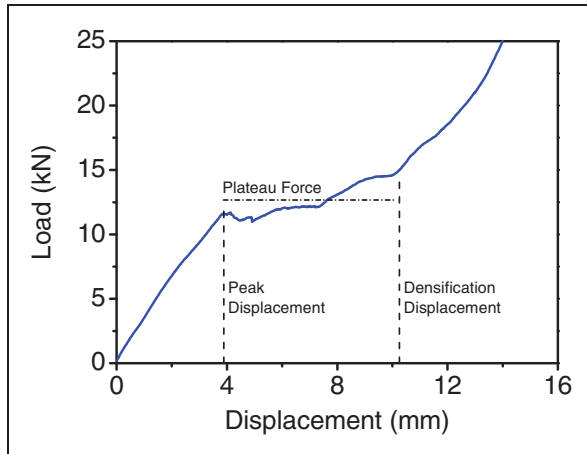
Figure 5. A typical indentation force–displacement curve of RS sandwich panels.

for simply supported (SS) and fully fixed (FF) sandwich panels, which will be discussed in the Effect of boundary conditions section. The force–displacement curves demonstrate the following key features. Load initially increases almost linearly to a peak load. After initial failure, at which the upper face sheet starts rupture, the load drops by a small amount, and then remains constant over a short flat plateau due to collapse of the cells. Note that the plateau is of great importance for energy absorption applications and the length of the plateau depends on the core thickness. Subsequently, the load increases again due to the back support edge effect.

To better compare the energy absorption of different structures, it is useful to use the so-called efficiency parameter to obtain indication for optimum usage of the structures. Referred to Avalle et al.,[22] the energy absorption efficiency is defined as

$$\eta(\delta) = \frac{1}{F(\delta)} \int_0^\delta F(\delta_1) \mathrm{d}\delta_1 \qquad (1)$$

where F is the indentation force and δ the indentation displacement. The densification displacement δ_d of sandwich panels under indentation is the displacement value corresponding to the stationary point in the efficiency–displacement curve where the efficiency is a global maximum:

$$\eta(\delta_d) = \max \eta(\delta) \qquad (2)$$

The plateau indentation force F_{pl} can be defined by

$$F_{pl} = \frac{1}{\delta_d - \delta_y} \int_{\delta_y}^{\delta_d} F(\delta) \mathrm{d}\delta \qquad (3)$$

where δ_y is the yield displacement corresponding to the displacement value at the first peak load. In this paper, the total energy absorption for the RS structures is defined as the area under the load–displacement curve up to densification displacement δ_d. However, it should be pointed out that this method can only be used for the RS boundary condition and cannot be used for SS and FF boundary conditions since there is no densification strain for SS and FF boundary conditions.

Discussion

Effect of face sheet thickness

In total, 18 RS sandwich panels were tested under the hemispherical indenter with three different face sheet thicknesses and three different core thicknesses. The specifications of the experiments and results are listed in Table 1, in which the energy absorption E is calculated from the area under the force–displacement curve up to the densification displacement and the specific energy absorption (SEA) is defined as the energy absorbed per unit mass. The energy-absorbing effectiveness factor Ψ is defined as the quotient of the total energy which can be absorbed in a system to the maximum failure energy in a normal tensile specimen made from the same volume of materials,[23,24] and it can be estimated from the following relation[18]

$$\Psi = \frac{\int_0^{\delta_d} F(\delta) \mathrm{d}\delta}{V_{uf} \int_0^{\varepsilon_r} \sigma_f \mathrm{d}\varepsilon + V_c \int_0^{\varepsilon_r} \sigma_c \mathrm{d}\varepsilon + V_{lf} \int_0^{\varepsilon_r} \sigma_f \mathrm{d}\varepsilon}, \qquad (4)$$

where F denotes the indentation force, δ the displacement of the indenter, δ_d the densification displacement, ε the uniaxial tensile strain, ε_r the uniaxial tensile engineering rupture strain of the composite face sheet (it is assumed that the maximum strain reached in the foam is equal to the uniaxial rupture strain of the face sheet material to simplify the analysis[23]), σ_f the static strength of the upper and lower face sheet material, σ_c the plateau crushing stress of the foam core, V_c the volume of the foam core, and V_{uf} and V_{lf} the volumes of the upper and lower face sheets, respectively. It is noted that the whole specimen was considered when calculating the volume.

Figure 6 shows the effects of upper face sheet thickness on the energy absorption performances of the RS sandwich panels under quasi-static indentation. As expected, the panels with thicker upper face sheets result in a higher force level and thus in higher energy absorption. For the range of thickness tested in this study, the energy absorption as well as the SEA is almost linearly proportional to the face sheet thickness. Table 1 indicates that by increasing the upper face sheet

Table 1. Experimental detail of specimens indented by hemispherical-nosed indenter (rigid back support; $\rho = 23.3\%$).

Specimen no.	Peak displacement (mm)	Peak loads (kN)	Densification displacement (mm)	Plateau loads (kN)	E (J)	SEA (J/kg)	Ψ	Damage mode
1.2-10-2.5-01	3.37	11.22	6.11	12.66	44.61	143.89	0.20	Mode-I
1.2-10-2.5-02	3.25	10.89	6.28	12.73	35.47	114.43	0.16	Mode-I
1.2-15-2.5-01	4.19	11.19	8.18	11.51	70.65	185.93	0.32	Mode-I
1.2-15-2.5-02	3.64	10.35	7.64	11.20	65.00	171.04	0.29	Mode-I
1.2-20-2.5-01	3.83	11.05	10.19	13.07	109.53	243.41	0.48	Mode-I
1.2-20-2.5-02	3.88	11.65	10.25	12.66	109.18	242.63	0.48	Mode-I
1.5-10-2.5-01	3.74	12.68	6.45	11.20	54.47	170.20	0.23	Mode-II
1.5-10-2.5-02	3.98	12.13	6.43	12.22	55.65	173.91	0.24	Mode-I
1.5-15-2.5-01	3.94	12.23	8.83	14.33	97.61	250.27	0.41	Mode-I
1.5-15-2.5-02	3.97	13.20	8.61	14.81	96.38	247.12	0.40	Mode-II
1.5-20-2.5-01	3.85	13.57	12.73	16.26	153.64	333.99	0.63	Mode-I
1.5-20-2.5-02	3.95	13.10	12.45	16.43	158.70	345.01	0.65	Mode-I
2.0-10-2.5-01	4.16	15.51	6.90	16.38	81.39	232.53	0.31	Mode-II
2.0-10-2.5-02	4.98	16.68	7.15	17.48	85.14	243.27	0.32	Mode-II
2.0-15-2.5-01	3.73	15.34	9.67	17.61	137.43	327.21	0.51	Mode-II
2.0-15-2.5-02	4.08	17.43	9.43	18.13	135.51	322.65	0.50	Mode-II
2.0-20-2.5-01	4.82	16.86	13.87	17.81	209.05	418.10	0.77	Mode-II
2.0-20-2.5-02	5.01	17.33	13.89	17.52	207.63	415.26	0.76	Mode-II
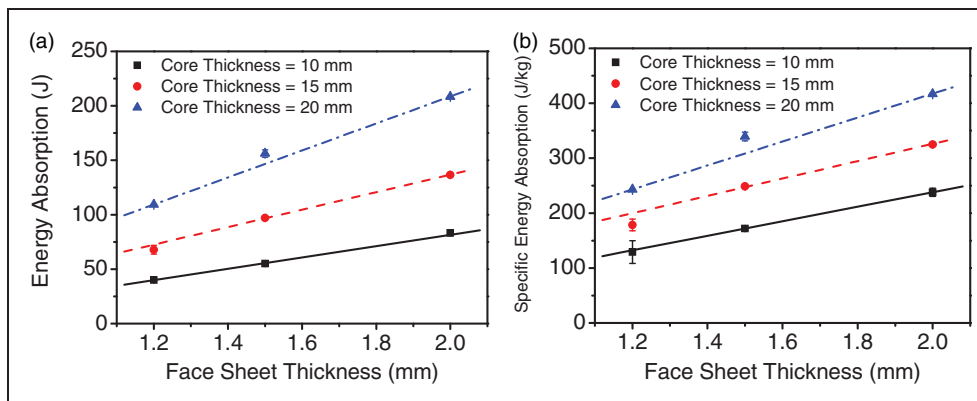
Figure 6. Effect of upper face sheet thickness on (a) energy absorption and (b) SEA (RS; hemispherical indenter; $\rho = 23.3\%$).

thickness the energy absorption efficiency of the sandwich panels with the same foam core thicknesses increases.

Effect of core thickness and core density

Figure 7 shows the effects of foam core thickness on the energy absorption performances of RS sandwich panels under quasi-static hemispherical indentation. The specifications of the panels and results are summarized in Table 2. As the indenter goes deeper, the aluminum foam core acts as an elastic-plastic foundation for the composite face sheets and it may affect the indentation responses of sandwich panels. Thus, foam core thickness shows a clear effect on the energy absorption of sandwich panels before failure. After upper face sheet failure, the foam core is crushed and densified as the indenter perforating into the foam core. The core thickness affects the plateau length of the force–displacement curve, which is also referred to as the densification displacement as mentioned above. Therefore, the core thickness is important especially in practical
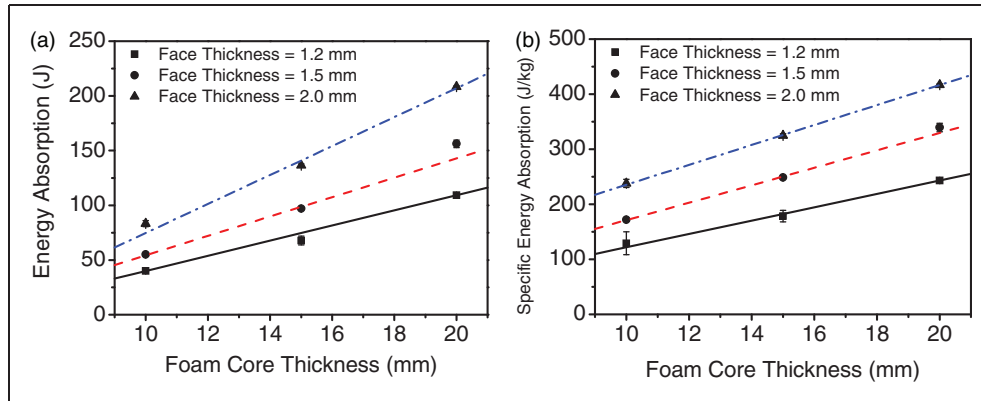
Figure 7. Effect of core thickness on (a) energy absorption and (b) SEA (RS; hemispherical indenter; $\rho = 23.3\%$).

Table 2. Experimental detail of specimens with different core densities indented by hemispherical-nosed indenter (rigid back support; $H_{uf} = 1.5$ mm; $H_{lf} = 2.5$ mm; $H_c = 15$ mm).

Specimen no.	Relative density (%)	Peak displacement (mm)	Peak loads (kN)	Densification displacement (mm)	Plateau loads (kN)	E (J)	SEA (J/kg)	Ψ	Damage mode
1.5-15-2.5-ρ1-01	14.1	4.40	12.38	8.28	11.84	76.22	245.86	0.32	Mode-I
1.5-15-2.5-ρ1-02	14.1	4.34	11.68	9.97	12.52	99.03	319.45	0.41	Mode-I
1.5-15-2.5-ρ1-03	14.1	4.08	11.30	9.44	12.14	91.87	296.35	0.38	Mode-I
1.5-15-2.5-ρ2-01	19.6	4.16	15.54	7.83	15.23	90.01	250.03	0.38	Mode-I
1.5-15-2.5-ρ2-02	19.6	4.37	14.38	8.73	16.38	107.45	298.46	0.45	Mode-I
1.5-15-2.5-ρ2-03	19.6	4.10	15.27	8.51	16.12	104.41	290.03	0.44	Mode-I
1.5-15-2.5-ρ3-01	23.3	4.09	16.49	8.00	18.75	110.46	283.24	0.46	Mode-II
1.5-15-2.5-ρ3-02	23.3	4.18	15.76	7.83	17.75	102.87	263.77	0.43	Mode-II
1.5-15-2.5-ρ3-03	23.3	3.92	17.49	8.33	19.32	122.32	313.65	0.51	Mode-II

applications such as sacrificial cladding structures, in which the foam core thickness will greatly affect the energy absorption. As can be seen in Figure 7, for sandwich panels with different face sheet thickness used in the present study, the energy absorption, SEA and energy absorption efficiency increase linearly as the foam core thickness increases.

Nine specimens with three different foam core relative densities ($\rho = 14.1\%$, 19.6% and 23.3%) were tested to study the effect of foam core density. All the specimens had identical face sheet thickness and foam core thickness ($H_{uf} = 1.5$ mm; $H_{lf} = 2.5$ mm; $H_c = 15$ mm) as well as the RS boundary condition. The results are listed in Table 2. A plot of the energy absorption performances of sandwich panels against their relative densities is shown in Figure 8.

Figure 8 reveals an approximate linear relationship between energy absorption, SEA of the sandwich
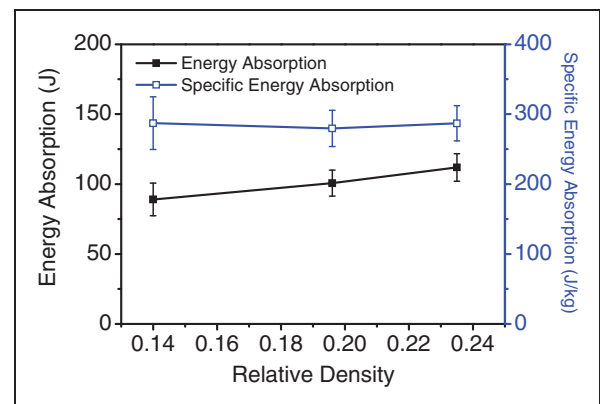

Figure 8. Effect of core density on energy absorption performances of RS sandwich panels ($H_{uf} = 1.5$ mm; $H_c = 15$ mm; hemispherical indenter).

panels, and the relative density of the foam core, respectively. These phenomena are because that higher density foam would result in a wider area to bear the indentation load, leading to a lower localized mean load. Higher density foams also show a higher load-carrying capacity and permit less deformation on the upper face sheets, which is favorable to energy absorption. It can also be found from Table 2 that the energy absorption efficiency of sandwich panels increases gradually as the relative density of the foam core increases.

Effect of indenter nose shape

The geometry of the indenter is a vital parameter that governs the indentation responses of sandwich panels.

Three indenters with different nose shapes, i.e. a conical-nosed punch (CNP), a hemispherical-ended punch (SEP) and a flat-ended punch (FEP), have been used in this study. Thirteen identical RS specimens were indented under quasi-static loading and the specifications of the panels and experimental results are listed in Table 3.

The photographs of the upper face sheets of the sandwich panels after tests are shown in Figure 3. It is obvious that the damage patterns of the upper face sheets depend on the geometry of the indenter. Blunt-nosed (hemispherical-nosed and flat-ended) indenters result in large damage areas.

The energy absorption performances of the sandwich panels indented quasi-statically are shown in Figure 9. The results indicate that sandwich panels

Table 3. Experimental details of specimens of identical configurations ($H_{uf} = 1.2$ mm; $H_{lf} = 2.5$ mm; $\rho = 23.3\%$) indented by indenters of different nose shapes.

| Specimen no.	Indenter shape	Peak displacement (mm)	Peak loads (kN)	Densification displacement (mm)	Plateau loads (kN)	E (J)	SEA (J/kg)	Ψ	Damage mode
1.2-10-2.5-01CN	CNP	2.37	2.22	4.62	1.99	8.24	26.58	0.04	Mode-VI
1.2-10-2.5-02CN	CNP	2.33	2.21	5.62	2.01	10.12	32.65	0.05	Mode-VI
1.2-10-2.5-01FE	FEP	1.66	26.19	4.55	20.78	90.61	292.28	0.41	Mode-III
1.2-10-2.5-02FE	FEP	1.39	25.79	4.84	21.37	98.28	317.03	0.45	Mode-III
1.2-10-2.5-03FE	FEP	1.05	26.11	5.16	23.34	112.37	362.48	0.51	Mode-III
1.2-10-2.5-01	SEP	3.37	11.22	6.11	12.66	54.61	176.15	0.25	Mode-I
1.2-10-2.5-02	SEP	3.25	10.89	6.28	12.73	57.47	185.40	0.26	Mode-I
1.2-20-2.5-01CN	CNP	2.29	2.68	5.12	2.53	11.47	25.48	0.05	Mode-VI
1.2-20-2.5-02CN	CNP	2.22	2.77	4.82	2.45	10.78	23.95	0.05	Mode-VI
1.2-20-2.5-01FE	FEP	1.73	25.93	9.86	22.65	216.93	482.07	0.96	Mode-III
1.2-20-2.5-02FE	FEP	1.65	26.55	9.31	22.66	206.33	458.52	0.91	Mode-III
1.2-20-2.5-01	SEP	3.83	11.05	10.19	13.07	105.53	234.52	0.47	Mode-I
1.2-20-2.5-02	SEP	3.88	11.65	10.25	12.66	105.18	233.74	0.46	Mode-I
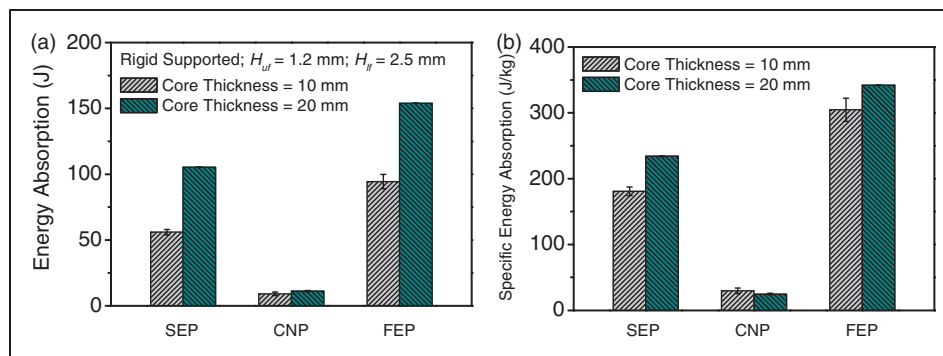
Figure 9. Effect of indenter nose shape on (a) energy absorption and (b) SEA of RS sandwich panels ($H_{uf} = 1.2$ mm; $H_{lf} = 2.5$ mm; $\rho = 23.3\%$).

perforated by the flat indenter (FEP) absorbed the most energy, followed by the hemispherical indenter (SEP) and then the conical indenter (CNP). So are the cases for SEA and energy-absorbing effectiveness factor. A possible explanation for this is that the damage mode-III resulted in an extremely high force level for the flat indenter cases, and more energy was absorbed. For the hemispherical indenter cases, much aluminum foam was compressed due to its relative large displacement before failure (Table 3), which caused more energy dissipation, while the conical indenter produced lower contact force and smaller deformation area, and less energy is dissipated during indentation.

Effect of boundary conditions

Boundary conditions can significantly affect the deformation behavior of structural members made from monolithic materials.[25] However, effects of boundary conditions on the responses of composite sandwich structures have been less documented. It is aimed in this section to obtain some information concerning the effect of boundary condition on the mechanical responses of composite sandwich panels. This was done with a hemispherical indenter by carrying out series tests on sandwich panels under three kinds of boundary conditions: placed on top of a rigid substrate support covering the entire area of the specimen without any clamping device (RS, Figure 2(a)), and placed on a specially designed frame with the edges of the specimen SS (Figure 2(b)) or with the edges of the specimen FF by eight bolts (FF, Figure 2(c)). The frame is made of steel and has a span of

$150 \times 150 \, mm^2$ with an exposed square ($90 \times 90 \, mm^2$) in the center and the fiber directions of the face sheets are parallel/perpendicular to the edges of the frame in the present experiments. Table 4 summarizes the test results and the force–displacement responses and energy absorption performances of the sandwich panels under different boundary conditions are shown in Figure 10.

Key features of the force–displacement responses as well as deformation and failure characteristics of the fully clamped sandwich panels have been studied previously. Two force peaks were found in the force–displacement curve corresponding to the upper and lower face sheet failure respectively. For more details, the reader is referred to our previous paper.[18] The values of E for the SS and FF cases are calculated from the area under the load–displacement curve up to the second peak load, which indicates the full failure of the sandwich panels. It is interesting to note that a much lower failure load is achieved for FF boundary condition due to the high degree of constraint. The upper face sheets of the FF sandwich panels were punched through around the circumferential edge of the indenter and cracks were produced in the lower face sheets along the edge of the frame over a larger area in a square manner that is parallel and perpendicular to the fiber direction under the indenter.[18] In contrast, the magnitude of the peak loads for SS sandwich panels is almost as large as that for RS panels. After the peak load, there is a long flat plateau, which allows large energy absorption at a constant load until a steep drop in force, indicating that the lower face sheet fails. Thus, RS panels absorb the greatest

Table 4. Experimental details of specimens of identical configurations ($H_{uf} = 2.0 \, mm$, $H_{lf} = 2.5 \, mm$; $\rho = 23.3\%$) indented under different boundary conditions.

| Specimen no.	Boundary condition	Peak displacement (mm)	Peak loads (kN)	Densification displacement (mm)	Plateau loads (kN)	E (J)	SEA (J/kg)	ψ	Damage mode
2.0-15-2.5-01	RS	3.73	15.34	9.67	104.61	137.43	327.21	0.51	Mode-II
2.0-15-2.5-02	RS	4.08	17.43	9.43	97.00	135.51	322.65	0.50	Mode-II
2.0-15-2.5-01SS	SS	8.66	17.56	–	–	109.56	260.86	0.41	Mode-II
2.0-15-2.5-02SS	SS	7.81	18.44	–	–	105.13	250.31	0.39	Mode-II
2.0-15-2.5-01FF	FF	26.28	5.59	–	–	97.16	231.33	0.36	Mode-II
2.0-15-2.5-02FF	FF	27.96	5.21	–	–	99.67	237.31	0.37	Mode-II
2.0-20-2.5-01	RS	4.82	16.86	13.87	161.19	209.05	418.10	0.77	Mode-II
2.0-20-2.5-02	RS	5.01	17.33	13.89	155.57	207.63	415.26	0.76	Mode-II
2.0-20-2.5-01SS	SS	10.27	15.87	–	–	130.86	261.72	0.48	Mode-II
2.0-20-2.5-02SS	SS	10.49	16.66	–	–	135.36	270.72	0.50	Mode-II
2.0-20-2.5-01FF	FF	32.20	4.92	–	–	117.41	234.82	0.43	Mode-II
2.0-20-2.5-02FF	FF	34.75	5.17	–	–	126.33	252.66	0.46	Mode-II
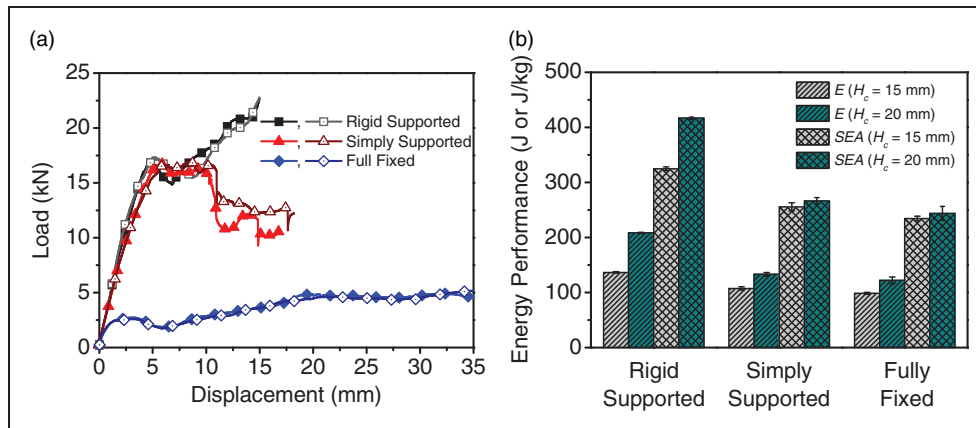
Figure 10. Effect of boundary conditions on energy absorption performances of RS sandwich panels (hemispherical indenter; $H_{uf} = 2.0$ mm; $H_c = 20$ mm; $\rho = 23.3\%$).

energy, own the highest SEA and energy absorption efficiency as well, while FF panels absorb the least energy and own the lowest SEA and energy absorption efficiency, as shown in Table 4 and Figure 10.

Conclusions

Quasi-static indentation tests are carried out to study the structural responses and energy absorption performances of sandwich panels with aluminum foam cores and composite face sheets. Most sandwich panels are indented by a hemispherical-nosed indenter, and two indenters with different nose shapes are also used for comparison purpose. The deformation and failure behaviors of sandwich panels are explored, and the energy absorption, SEA, and energy absorption efficiency of different structures are investigated and compared.

Based on the quantitative results obtained, the effects of several key parameters, including the face sheet thickness, the foam core thickness and relative density, and the indenter nose shapes, on the energy absorption performances of the sandwich panels under indentation are discussed. Thicker face-sheet, thicker or denser foam core are prone to producing higher energy absorption and resulting in higher energy absorption efficiency. The sandwich panels perforated by a flat indenter absorb the most energy with the highest energy-absorbing efficiency, while a conical indenter gives the lowest penetration load, the lowest energy absorption, and the lowest energy absorption efficiency. A dependency of the indentation response on the boundary conditions is also observed. The RS sandwich panels absorb the greatest energy and own the highest energy absorption efficiency, while FF panels absorb the least energy and own the lowest energy absorption efficiency.

Conflict of interest

None declared.

References

1. Zenkert D. *An introduction to sandwich construction.* Sheffield: Engineering Materials Advisory Services, 1995.
2. Abrate S. *Impact on composite structures.* Cambridge: Cambridge University Press, 1998.
3. Ugale VB, Singh KK, Mishra NM, et al. Experimental studies on thin sandwich panels under impact and static loading. *J Reinf Plast Compos* 2013; 32: 420–434.
4. Zhu S and Chai GB. Damage and failure mode maps of composite sandwich panel subjected to quasi-static indentation and low velocity impact. *Compos Struct* 2013; 101: 204–214.
5. Chai GB and Zhu S. A review of low-velocity impact on sandwich structures. *Proc Inst Mech Eng L – J Mater* 2011; 225: 207–230.
6. Hachemane B, Zitoune R, Bezzazi B, et al. Sandwich composites impact and indentation behaviour study. *Compos Part B* 2013; 51: 1–10.
7. Baştürk SB and Tanoğlu M. Mechanical and energy absorption behaviors of metal/polymer layered sandwich structures. *J Reinf Plast Compos* 2011; 30: 1539–1547.
8. Flores-Johnson EA and Li QM. Experimental study of the indentation of sandwich panels with carbon fibre-reinforced polymer face sheets and polymeric foam core. *Compos Part B* 2011; 42: 1212–1219.
9. Sezgin FE, Tanoğlu M, Eğilmez OÖ, et al. Mechanical behavior of polypropylene-based honeycomb-core composite sandwich structures. *J Reinf Plast Compos* 2010; 29: 1569–1579.

10. Yang M, Qiao P and Asce F. Quasi-static indentation behavior of honeycomb sandwich materials and its application in impact simulations. *J Aerospace Eng* 2008; 21: 226–234.

11. Ruan D, Lu G and Wong YC. Quasi-static indentation tests on aluminium foam sandwich panels. *Compos Struct* 2010; 92: 2039–2046.

12. Mohan K, Yip TH, Sridhar I, et al. Effect of face sheet material on the indentation response of metallic foams. *J Mater Sci* 2007; 42: 3714–3723.

13. Zhou J, Hassan MZ, Guan Z, et al. The low velocity impact response of foam-based sandwich panels. *Compos Sci Technol* 2010; 72: 1781–1790.

14. Xie ZY, Zheng ZJ and Yu JL. Localized indentation of sandwich beam with metallic foam core. *J Sandw Struct Mater* 2012; 14: 197–210.

15. Harte AM, Fleck NA and Ashby MF. Sandwich panel design using aluminum alloy foam. *Adv Eng Mater* 2000; 2: 219–222.

16. Flores-Johnson EA. Quasi-static indentation and low velocity impact on polymeric foams and CFRP sandwich panels with polymeric foam cores. PhD thesis: The University of Manchester, Manchester, 2009.

17. Nettles AT and Douglas MJ. A comparison of quasi-static indentation testing to low velocity impact testing. *Compos Mater: Test Des Accept Crit* [ASTM STP 141] 2002; 1416: 116–130.

18. Li ZB, Zheng ZJ and Yu JL. Low-velocity perforation behavior of composite sandwich panels with aluminum foam core. *J Sandw Struct Mater* 2013; 15: 92–109.

19. Bažant ZP, Zhou Y, Daniel IM, et al. Size effect on strength of laminate-foam sandwich plates. *J Eng Mater Tech* 2006; 128: 366–374.

20. Andrews EW, Gioux G, Onck P, et al. Size effects in ductile cellular solids. Part II: Experimental results. *Int J Mech Sci* 2001; 43: 701–713.

21. Tekoglu C, Gibson LJ, Pardoen T, et al. Size effects in foams: Experiments and modeling. *Prog Mater Sci* 2011; 56: 109–138.

22. Avalle M, Belingardi G and Montanini R. Characterization of polymeric structural foams under compressive impact loading by means of energy-absorption diagram. *Int J Impact Eng* 2001; 25: 455–472.

23. Jones N. Energy-absorbing effectiveness factor. *Int J Impact Eng* 2010; 37: 754–765.

24. Li ZB, Yu JL and Guo LW. Deformation and energy absorption of aluminum foam-filled tubes subjected to oblique loading. *Int J Mech Sci* 2012; 54: 48–56.

25. Jones N. *Structural impact*. Cambridge: Cambridge University Press, 1997.